

Research Article

Andrew Boyd*, Michael Ponting and Howard Fein

Layered polymer GRIN lenses and their benefits to optical designs

DOI 10.1515/aot-2015-0035

Received June 25, 2015; accepted August 12, 2015; previously published online September 8, 2015

Abstract: We discuss the findings of a recent optical design study into layered polymeric gradient index lenses (known as L-GRIN). A range of GRIN singlet lenses were designed for various aperture and field-of-view configurations. Their optical performance was compared to polymer diffractive lenses and glass-cemented doublets (both spherical and aspheric) designed to the same specification. We find that diamond-turned polymer GRIN lenses offer comparable performance to achromatic doublets and polymer diffractive hybrid elements over a significant aperture and field-of-view range. We also find that the correction potential of GRIN solutions is substantially increased when the bulk GRIN Abbé value (V_{10}) is negative, the GRIN distribution is radial, or the index range (ΔN) of the GRIN is increased significantly.

Keywords: color correction; GRIN; L-GRIN; optical design.

1 Introduction

It is of key interest in the imaging optics industry to generate products that provide good image quality at reduced size mass and cost. Optical design lies central to this; opto-mechanical modules often comprise the majority of the size and mass of an imaging system.

Traditionally, optical systems have used one of three methods to correct chromatic and spherical aberrations (Figure 1). First, the classical doublet enables color correction through balancing the wavelength-dependent powers

of two lenses of different materials cemented together. It is a well-understood and effective solution but involves the use of glass lenses, which are heavier than polymer lenses and requires that two lenses be made and precisely aligned through a cementing operation. Second, a hybrid diffractive lens enables color correction through the use of a highly dispersive blazed surface. This blaze can be diamond turned onto a polymer substrate enabling the generation of a lightweight, well-corrected solution, which is easy to manufacture. However, diffractive lenses have limitations due to the stray light effects of spurious diffraction orders, which can become problematic in broad wavebands or high dynamic range scenarios. A GRIN lens made from a polymer substrate has the potential to reduce the mass of an optical system by eliminating denser glass material while simultaneously enabling correction in requirements that are unsuitable to diffractive optics.

The primary barrier to widespread adoption of GRIN technology has been the cost and complexity of manufacture. Recent developments in layered polymer GRIN technology (known as L-GRIN) have the potential to overcome this barrier.

Developed over the past decade, L-GRIN materials rely on the forced assembly of a very large number of sub-wavelength polymer films of two or more different refractive indices [1]. Owing to their negligible optical thickness, the layers act as an effective medium for visible or longer wavelengths. By controlling the relative thicknesses of the fixed-index alternating layers, the refractive index of the medium can be modified spatially. This approach enables the generation of polymer lens preforms with axial, spherical, and even aspheric GRIN profiles. The polymers currently used to generate L-GRINS (PMMA and SAN17) are suitable for single-point diamond turning (SPDT). This enables economical generation of aspheric surfaces on the finished lens. These surfaces need not necessarily be conformal with the polymer nano-layers.

The L-GRIN manufacturing process is summarized in Figures 2 and 3 [2]. Two materials are co-extruded through a layer-multiplying process to generate 50- μm -thick films of constant, yet customizable, refractive index. Index

*Corresponding author: Andrew Boyd, Qioptiq, Glascoed Road, St Asaph, Denbighshire, LL170LL, UK, e-mail: andrew.boyd@uk.qioptiq.com

Michael Ponting and Howard Fein: Polymerplus Inc., 7700 Hub Parkway, Valley View, OH 44125, USA

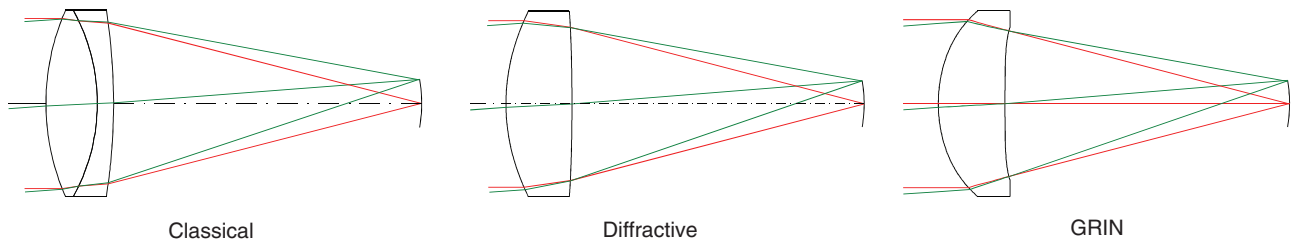


Figure 1: Three methods of correcting optical aberrations: a classical doublet, hybrid diffractive lens, and GRIN.

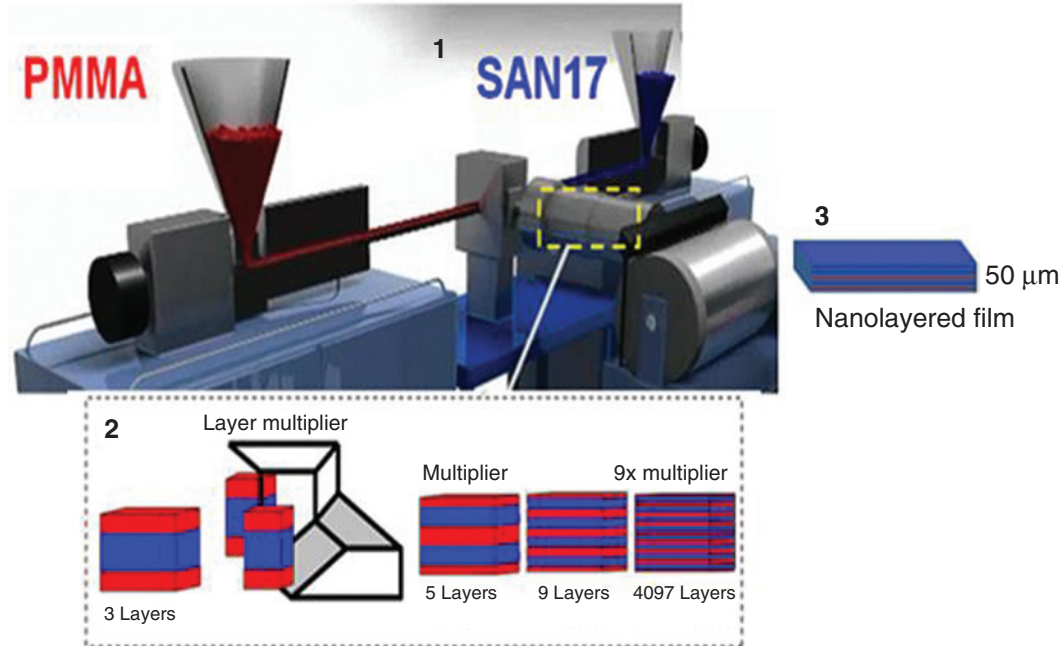


Figure 2: The PolymerPlus co-extrusion process.

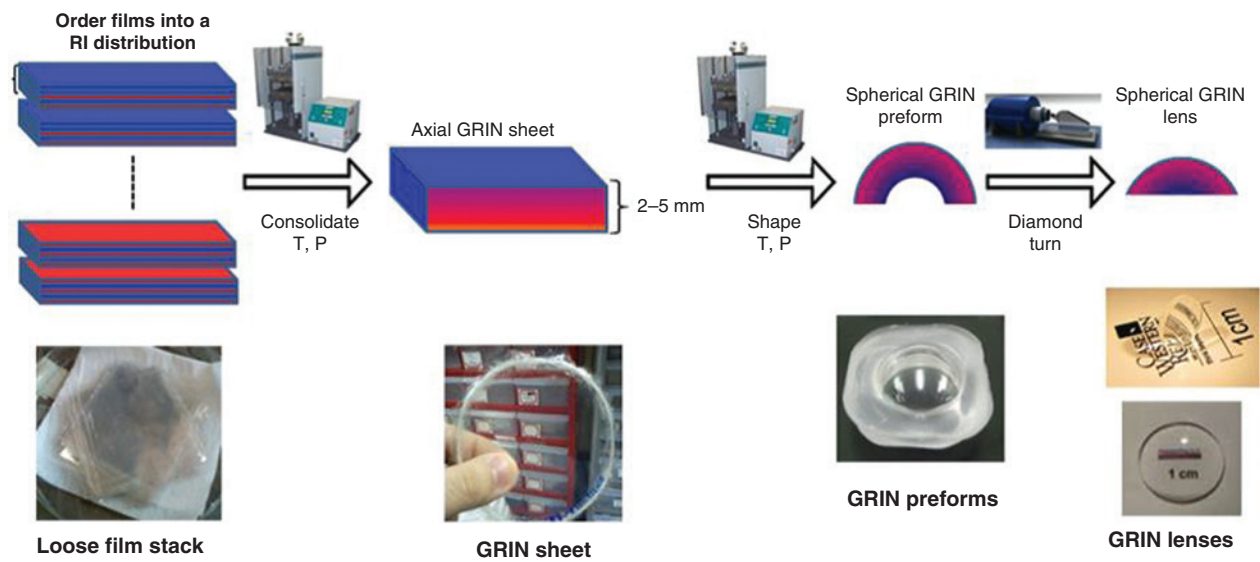


Figure 3: Schematic of the L-GRIN production process.

customization is achieved by varying the proportional thickness of the input layers via inline precision melt pumps calibrated to control the relative polymer material feed rates down to 0.3%. Quality assurance refractive index testing is routinely performed on processed 475-m long \times 0.5-m wide nano-layered film rolls to ensure the target refractive index is achieved. Based on the developed nano-layered film refractive index testing procedures averaged from 750 unique measurements over the entire roll, a refractive index variation tolerance of $<2.5 \times 10^{-4}$ must be met to qualify the material for continued processing into GRIN optics. Once qualified, these films are then used to populate an inventory of available index values. The films are then selected and stacked subject to the design of the GRIN profile. This film stack is then consolidated into a single GRIN sheet. From here, the axial GRIN may be molded further into a spherical (potentially non-spherical) GRIN preform. The optical surface quality of the spherical preforms is sufficient to allow optical alignment of preforms to diamond turning lathes.

Polymer GRINs are not subject to the same manufacturing constraints that diffusion-driven GRIN manufacture methods are limited by. This novel method of GRIN manufacture requires a new optical design modeling approach. A simple spherical GRIN formalism can be defined as follows:

$$N(R) = N_0 + N_1 R + N_2 R^2 + N_3 R^3 + \dots$$

where $R^2 = x^2 + y^2 + z^2$

This enables the index to vary from a GRIN origin whose coordinate system may be decoupled from that of the optical geometry (i.e. the origin of the GRIN geometry need not necessarily sit within the lens itself).

In the case of a pressed polymer GRIN, there is also no mathematical requirement that the origin of the index polynomial resides at the origin of the GRIN geometry. With this in mind, we can effect a coordinate transformation to ease the design process. This greatly aids the optical design process, as without it, the polynomial terms required to meet a given GRIN distribution become much more complex making solutions hard to reach through optimization.

Figure 4 shows how the index variation may be defined in a coordinate system based on local radius (R_{loc}). The GRIN contour origin lies outside the lens; this is the center of curvature of the mold, which will be used to manufacture a GRIN blank. All the contours of our GRIN, therefore, need to be concentric to this point. Y_{len} and Z_{len} represent the local surface Cartesian coordinates of a ray inside a GRIN as will generally be requested by commercial optical design software such as CodeV® (Synopsys

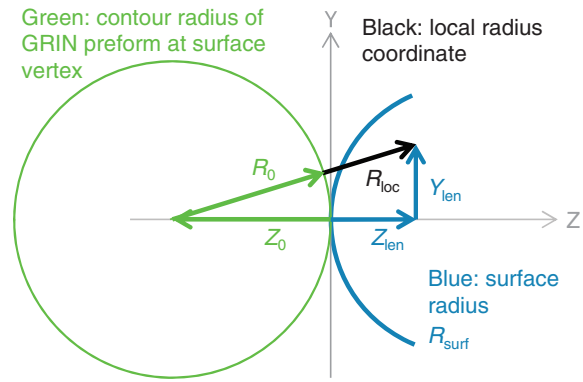


Figure 4: Schematic of the required coordinate transform to model a spherical polymer GRIN.

Inc., Pasadena, CA, USA) or Zemax® (Zemax LLC, Kirkland, WA, USA). From Figure 4, we can now define R and R_{loc} as:

$$R_{contour} = R_{loc} + R_0, \text{ where } R_0 = -z_0$$

$$R_{contour}^2 = x_{len}^2 + y_{len}^2 + (z_{len} - z_0)^2$$

We then change the variable of our GRIN polynomial to R_{loc} :

$$N(R_{loc}) = N_0 + N_1 R_{loc} + N_2 R_{loc}^2 + N_3 R_{loc}^3 + \dots$$

The coordinate transformation has now decoupled the origin which controls the contour curvature from the origin which controls the index polynomial. Our new local coordinate allows us to use much lower-order polynomials to express complicated GRIN distributions over the volume of a lens, regardless of the value of Z_0 .

In order to model accurately a GRIN lens made from any two known materials (say A and B), one must also consider chromatic dispersion effects. L-GRIN can be modeled as a mixture of the two constituent materials where the index varies linearly with the volumetric proportion of each material between the properties of A and B (Figure 5).

Owing to the fact that this index change is linear, it is possible to generate a wavelength-dependent scaling coefficient, defined as the ratio of the index change at a given wavelength to the index change at a reference wavelength. It is worth noting at this point that any GRIN distribution for chromatically dispersive materials is not meaningful unless it is specified for a given reference wavelength.

$$C(\lambda) = \frac{\Delta N(\lambda)}{\Delta N(\lambda_{ref})}, \text{ where } \Delta N(\lambda) = N_{0B}(\lambda) - N_{0A}(\lambda)$$

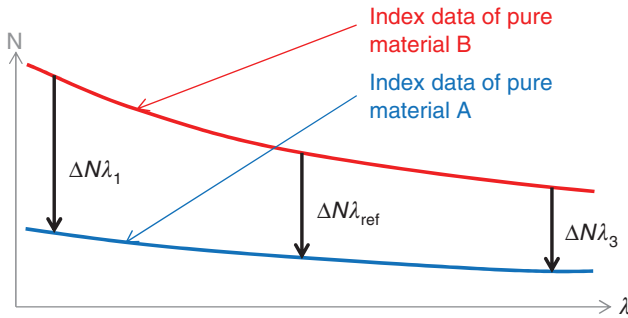


Figure 5: GRIN index scaling between hypothetical materials A and B.

Our index distribution with wavelength is now:

$$N(R_{loc}, \lambda_n) = N_{0A}(\lambda_n) + C(\lambda_n)[N_0 + N_1 R_{loc} + N_2 R_{loc}^2 + N_3 R_{loc}^3]$$

For optimization, it is useful to add a variable N_0 term; this essentially changes the starting material at $R_{loc}=0$. An N_0 value equal to $\Delta N(\lambda_{ref})$ represents a full transition to material B while retaining the correct dispersion properties. The index variation generated by the bracketed term must be constrained to within $\Delta N(\lambda_{ref})$ over a GRIN lens volume to avoid the design of an unmanufacturable material.

2 GRIN lens color correction

GRIN lenses are capable of correcting chromatic aberrations. This occurs via a similar mechanism to that of an achromatic doublet. GRIN color correction can be split into one of two mechanisms:

2.1 Surface GRIN

Color correction takes place on the lens surfaces themselves. This correction is best demonstrated by an axial GRIN distribution. An axial index gradient has no power in itself, but a change in dispersion along the optical axis between the front and rear surface of the lens allows color correction to take place. Using our example materials of A and B from Figure 5, we can show how an achromatic design can be generated (Figure 6). In our example, material B (shown in red) has greater dispersion than material A (blue), i.e. $V_A > V_B$. The power of each surface is dependent upon the surface curvature. An analogous condition to that of a conventional doublet applies as follows:

$$\frac{K_{s1}}{V_A} + \frac{K_{s2}}{V_B} = 0$$

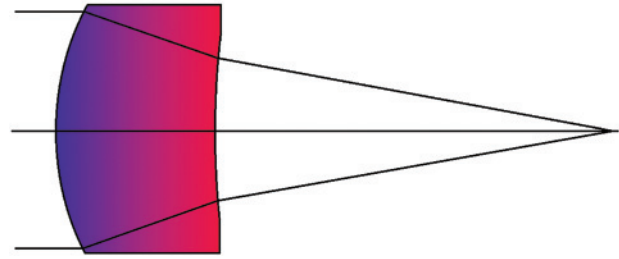


Figure 6: Schematic of an achromatic axial GRIN composed of hypothetical materials A and B.

There is a large amount of positive power with low dispersion on surface 1 and a smaller amount of high dispersion negative power on surface 2.

2.2 Transfer GRIN

Color correction takes place between surfaces, i.e. within the GRIN itself. This is demonstrated most simply using a radial GRIN distribution (i.e. index variation perpendicular to the optical axis). If an arbitrary radial GRIN is decomposed into a number of polynomial terms, the coefficient of the second power of aperture radius represents the GRIN power:

$$N(\rho) = N_0 + N_1 \rho^2 + N_2 \rho^4 + N_3 \rho^6 + \dots$$

where $\rho^2 = x^2 + y^2$ and z are parallel to the optical axis.

The GRIN power term, itself, varies with wavelength due to the fact that the ΔN of a specific material pairing itself varies with wavelength. This gives rise to a GRIN Abbé term [3] as follows:

$$V_{10} = \frac{\Delta N_{\lambda_{mid}}}{\Delta N_{\lambda_{short}} - \Delta N_{\lambda_{long}}}$$

This Abbé term can be highly dispersive. For example, two polymers commonly used for L-GRINs are polymethyl methacrylate (acrylic) or styrene acrylonitrile (SAN17). In isolation, these have Abbé V_{00} values of 46.34 and 23.64, respectively. When combined as a GRIN, this resulting material has a V_{10} value of 6.16. A radial GRIN lens can now provide positive, achromatic focusing power to the optical system using a combination of the lens surfaces and weak, high dispersion power from the GRIN. This again leads to a similar achromatism condition:

$$\frac{K_{s1}}{V_{00}} + \frac{K_{s2}}{V_{00}} + \frac{K_{GRIN}}{V_{10}} = 0, \text{ where } V_{00} = \frac{N_{axis \lambda_{mid}}}{N_{axis \lambda_{short}} - N_{axis \lambda_{long}}}$$

The power term, K_{GRIN} , of a radial GRIN is given by: $K_{GRIN} = -2N_1t$, where t is the lens thickness along the optical axis.

Spherical GRIN distributions correct color using a combination of these two methods, as a spherical GRIN generates both axial and radial variation in refractive index. The variation along the optical axis and perpendicular to it are coupled, due to the contoured nature of the spherical GRIN formalism.

3 Trade study parameters

To investigate the aberration correction properties of L-GRIN lenses, we undertook trade studies into the performance of

Table 1: Basic trade study lens specification.

Parameter	Value(s)
Focal length	50 mm
Entrance pupil diameter (EPD)	5, 10, 15, 20, 25 mm
Field of view	0, 4, 8°
Waveband	450–650 nm, uniform spectral weighting
Image plane	Curved image permitted
Lens thickness	10 mm max
RMS spot size	To be minimised

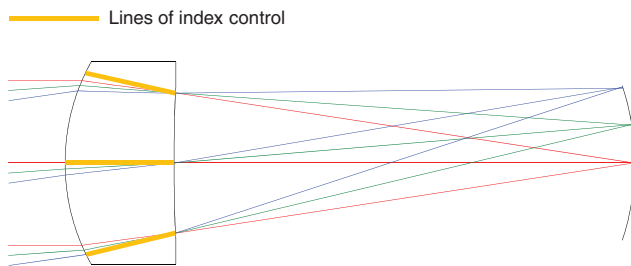


Figure 7: Regions of a GRIN lens where the index is constrained in optimization.

simple, single element systems of various F-number and field-of-view configurations. A set of GRIN, spherical doublet, aspheric doublet and diffractive lenses were designed according to a basic specification listed in Table 1.

The material combination used for the GRIN lenses was PMMA-SAN17 ($\Delta N=0.085$, $V_{10}=6.16$). The effectiveness of GRIN lenses is heavily dependent upon the lens thickness; therefore, to ensure a fair comparison between lenses, the axial thicknesses of each lens were limited to 10 mm.

4 Optimization process

Material selection for the glass doublets was limited to commercially available glass. The CodeV® macro *glassexpert.seq* was used to quickly and accurately find the optimal glass choice, thicknesses, and curvatures over the full range of fields and apertures of the trade study (30 glass designs in total). The material pairings chosen were required to be thermally stable by means of a tolerance on glass CTE mismatch. Any doublet that demonstrated a deviation $>0.1 \mu\text{m}/^\circ\text{C}$ over the clear aperture was rejected.

The trial GRIN lenses were optimized using the CodeV® automatic design (AUT) option. It was necessary to control the refractive index limits of the GRIN lenses during optimization to prevent unmanufacturable solutions from being generated. This was done via user-defined functions within optimization itself. Maximum and minimum refractive index limits were defined as the pure forms of each constituent material of the GRIN. At 550 nm, the refractive indices of PMMA and SAN17 were modeled as 1.4936 and 1.5788, respectively. For the sake of computational simplicity, the refractive index profile was controlled along the optical axis and at the clear aperture (Figure 7). This method of control was generally effective, as index extremes within GRIN lenses tended to occur along the optical axis and at the outer

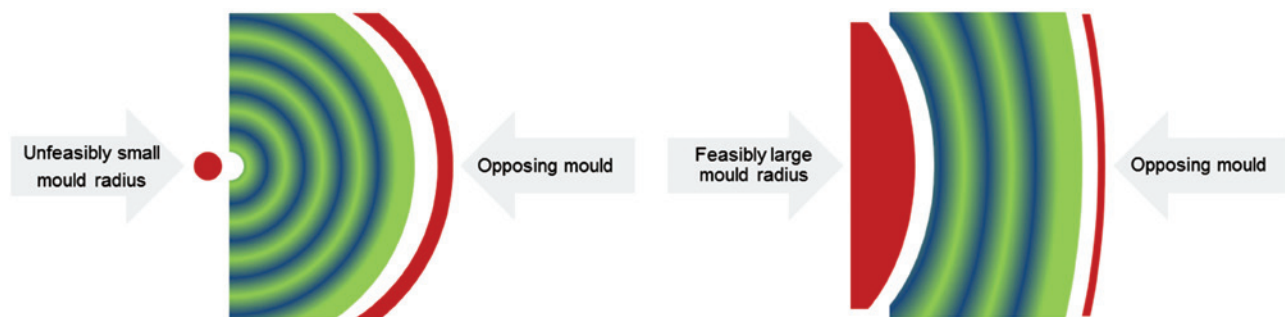


Figure 8: Large and small mould radius scenarios.

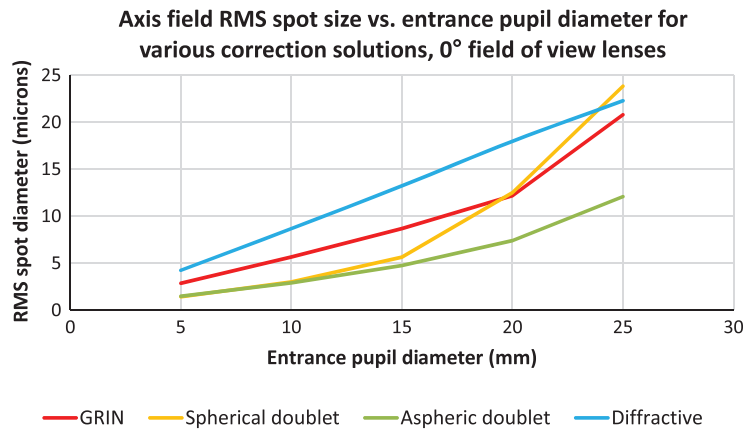
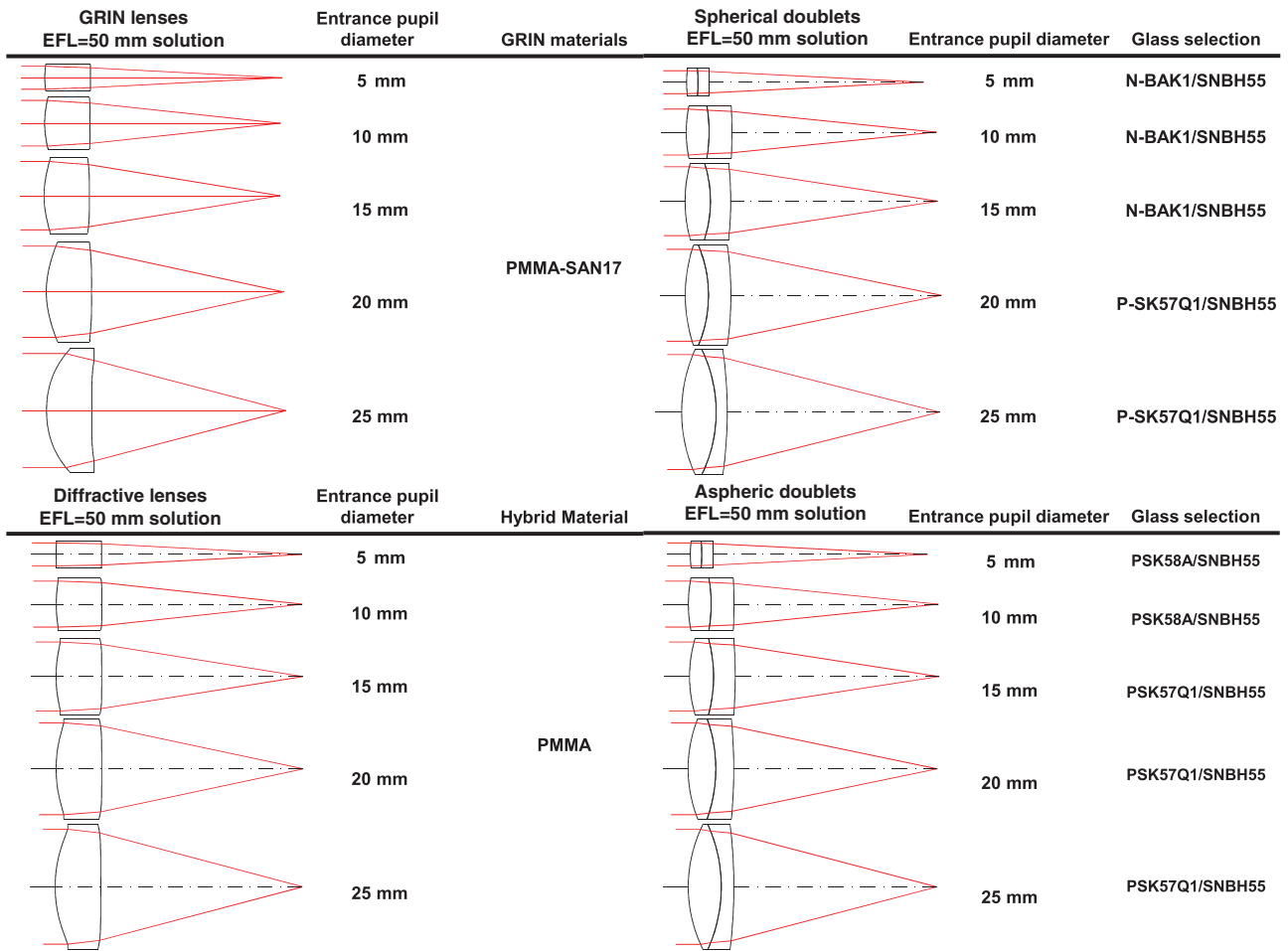


Figure 9: Trade study lens designs and RMS spot sizes for the axial specification.

aperture. This index control process was further simplified by the fact that we have rotational symmetry within our system.

It was also important to control the GRIN contour origin offset, z_0 . Left unconstrained, this had a tendency

to produce solutions with the origin of the GRIN contours internal to the lens itself, which is unfeasible to manufacture via a molding process. A basic molding feasibility constraint was added, which did not allow the GRIN curvature origin, z_0 , any closer to the lens vertex than the

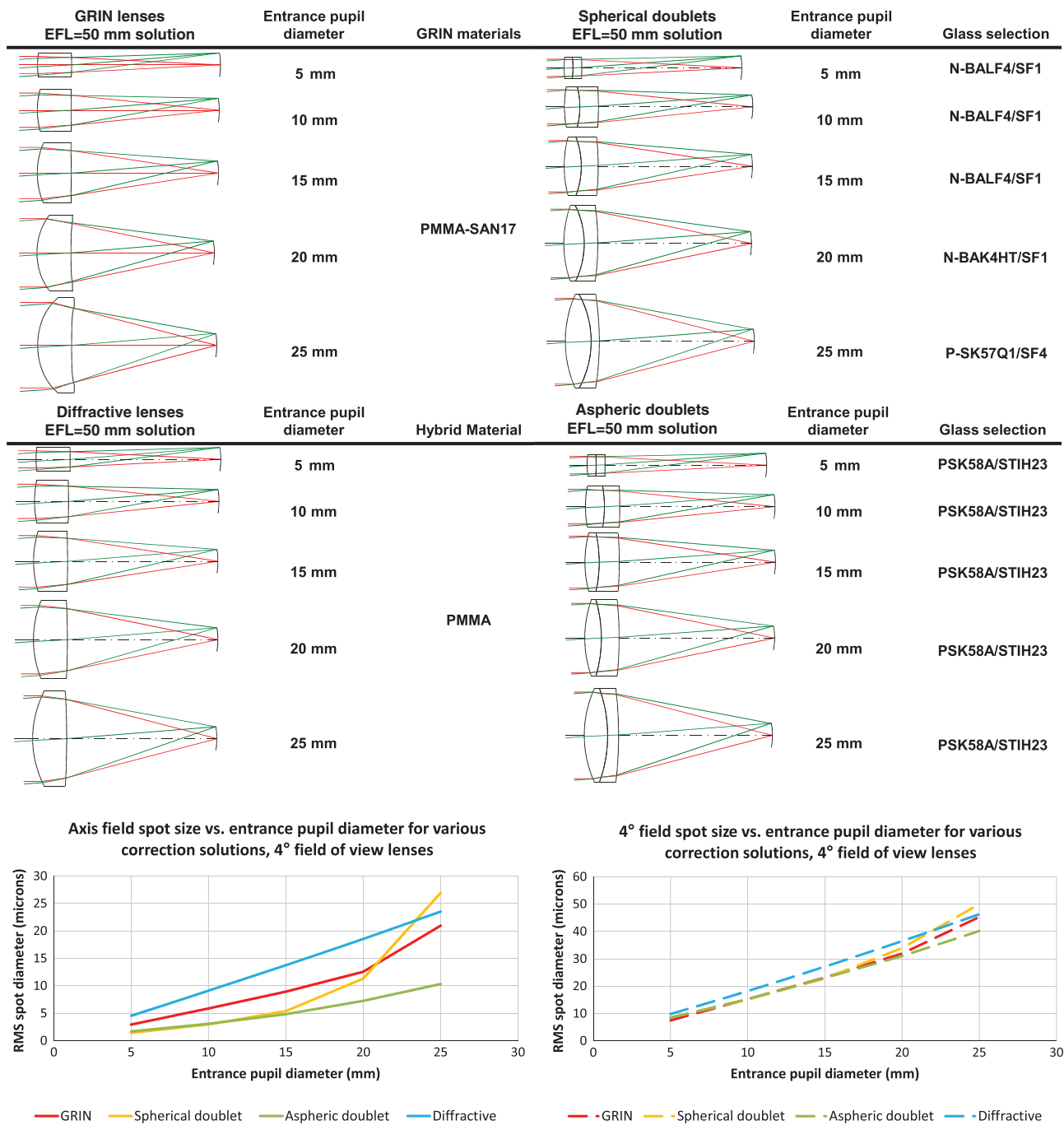


Figure 10: Trade study optical designs and RMS spot sizes for the 4° field-of-view specification.

size of the adjacent clear semi-aperture. This avoids the scenario shown on the left-hand side of Figure 8.

Finally, as both surfaces of the GRIN lens are diamond turned, we can allow aspheric terms to combine with the GRIN properties to correct aberrations. The number of variable aspheric terms was increased progressively until the optimization process stagnated.

5 Results

The RMS spot size over the field of view was recorded for each trade space lens. The lens designs and RMS spot size values are shown in Figures 9–11.

We observe nonlinear growth in the axial RMS spot size vs. the EPD of each solution type with the exception

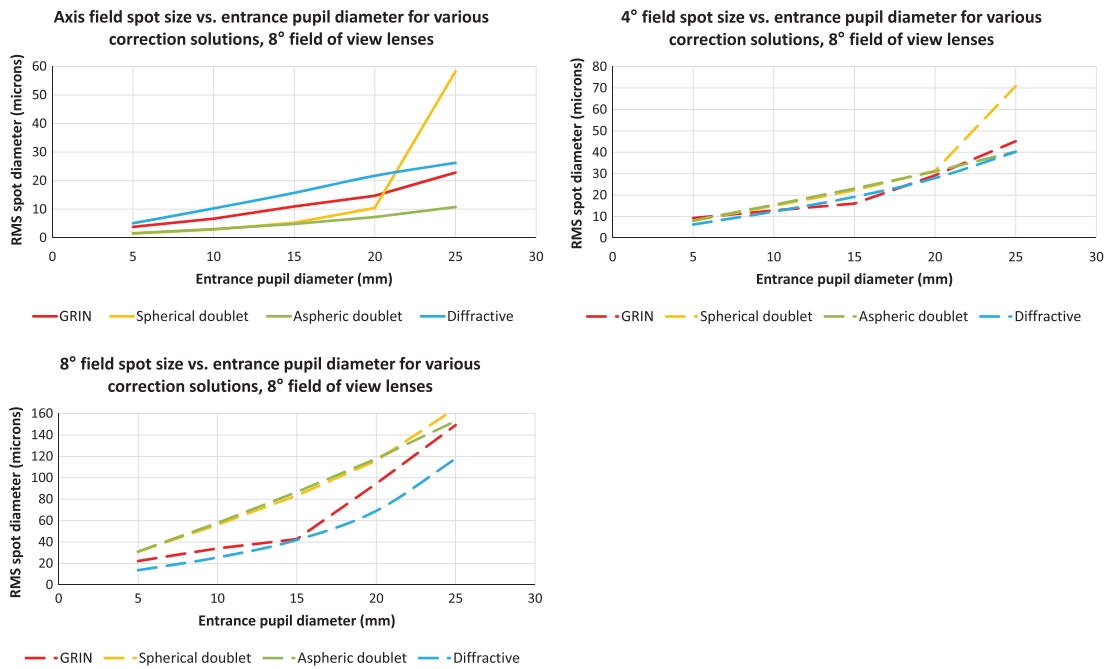
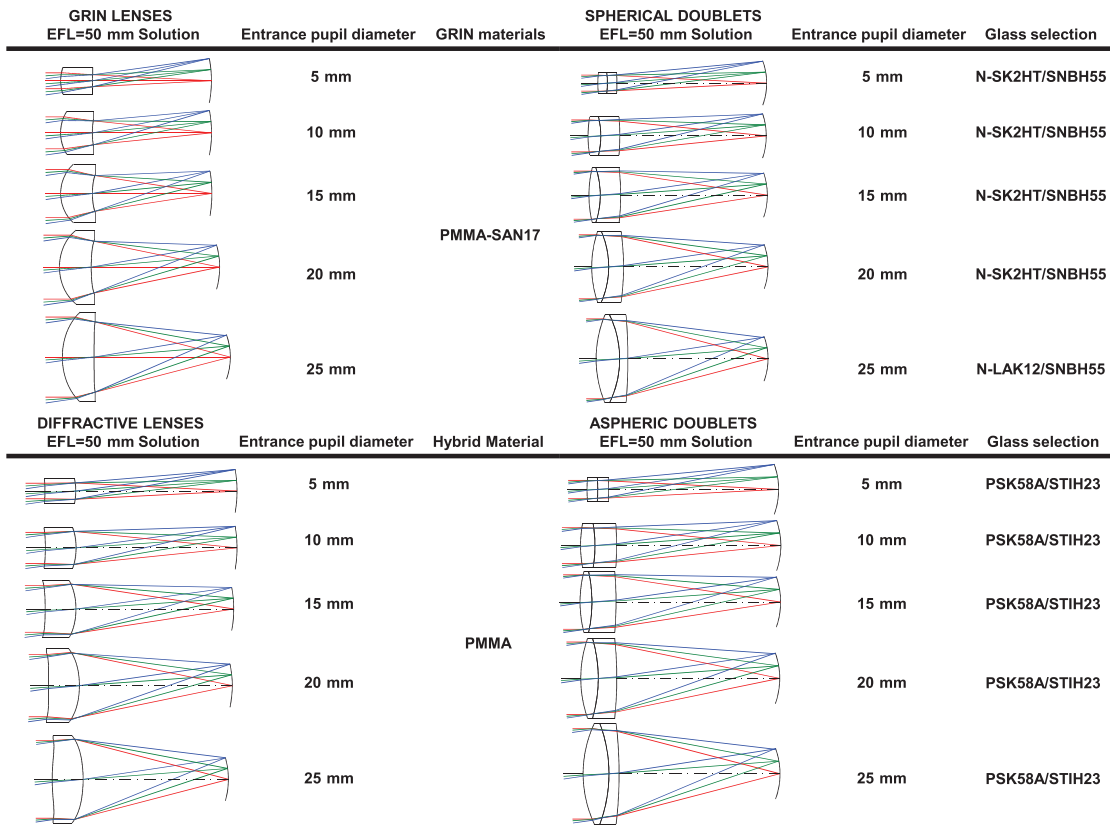


Figure 11: Trade study optical designs and RMS spot size for the 8° field-of-view specification.

of the diffractive solution. Particularly rapid growth is seen in the spot size of the spherical doublet solutions. At the edge of the field of view, the performance of each

solution type is broadly similar. For the widest angle solutions with a field of view of 8°, some greater variation in spot size is observed with the diffractive and GRIN lenses

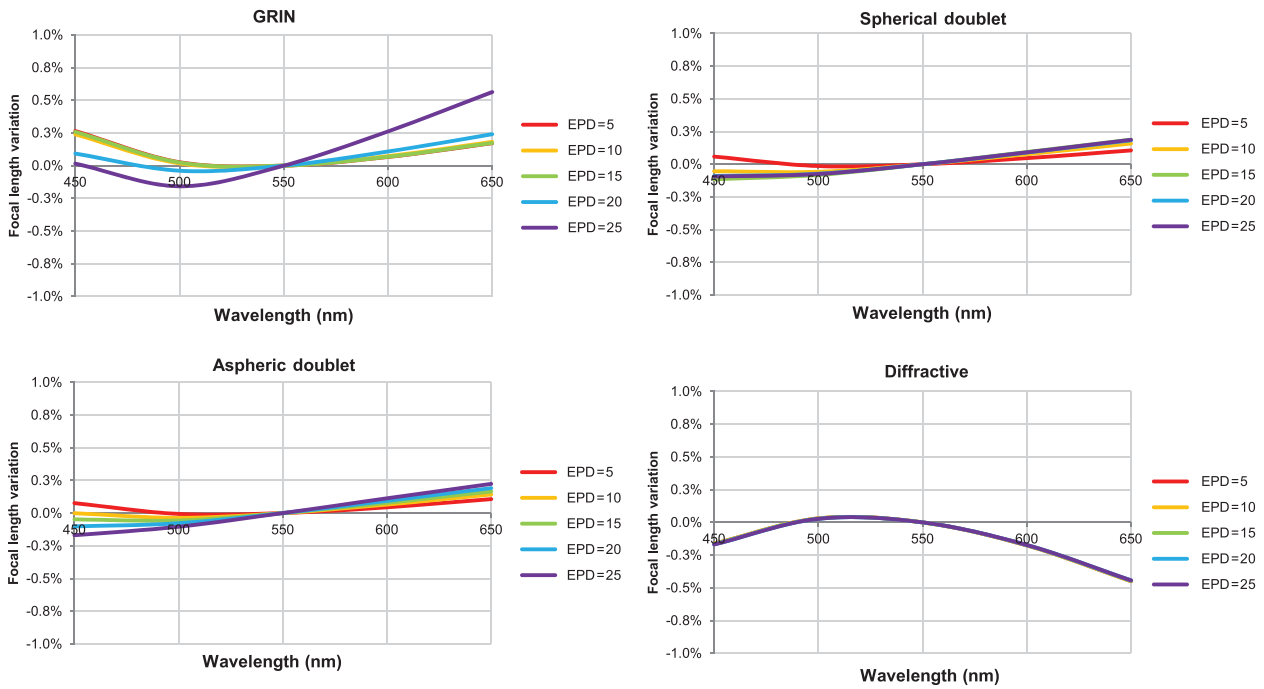


Figure 12: Percentage focal length variation of axial field 50-mm designs.

Axial transverse errors of GRIN, hybrid and doublet 4° singlets (mm)

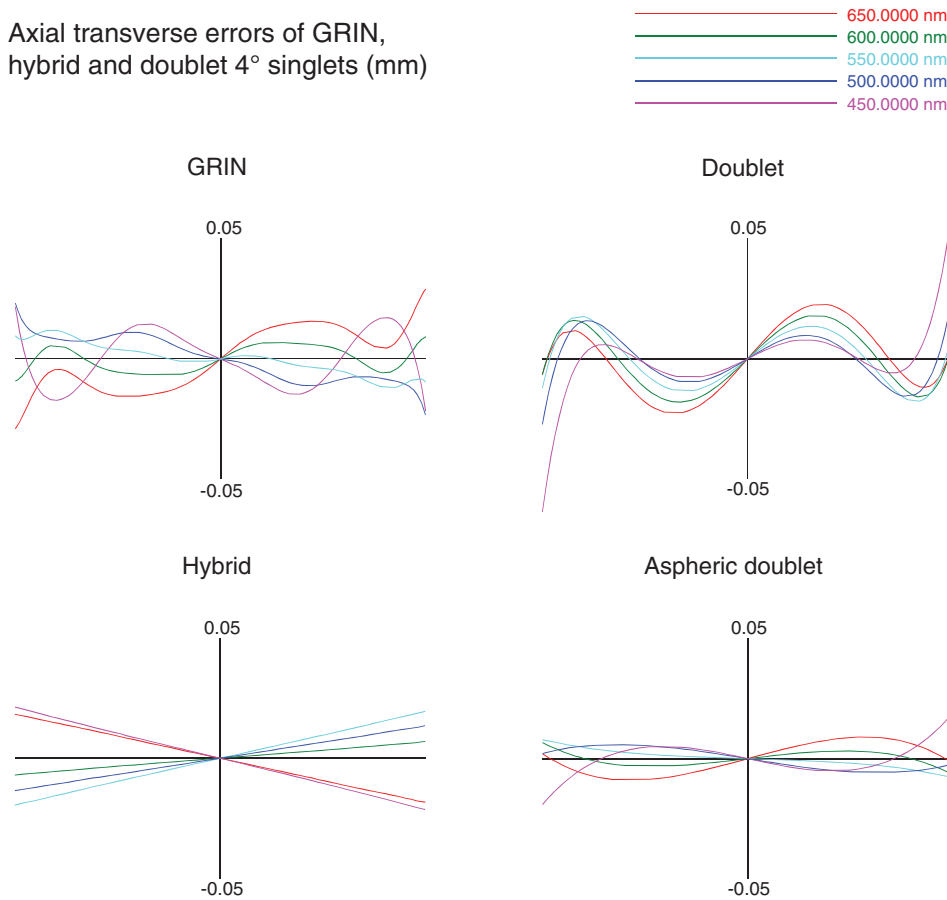


Figure 13: Transverse ray aberrations of GRIN, doublet, diffractive, and aspheric doublet 4° FOV designs (EPD=25 mm).

outperforming the doublet lenses. The spherical doublets show particularly rapid growth in on-axis spot size due to the onset of spherical aberration.

As color correction is a key objective of GRIN lens usage, the percentage variation of the focal length against wavelength was recorded for each solution type (Figure 12).

We observe achromatic correction from the GRIN distribution for the 5 mm, 10 mm, and 15 mm EPD lenses. This comes in the form of a ‘U’-shaped variation of focal length with wavelength. Beyond 15 mm EPD, we begin to see a breakdown in the level of correction. The variation of focal length with wavelength becomes gradually more ‘hockey stick’ shaped, with a progressively smaller region of the waveband corrected for two wavelengths. Chromatic aberration remains well controlled by both the spherical and the aspheric doublets over the full aperture range. The diffractive solution shows a fixed level of secondary spectrum for all EPD values. Note that the secondary spectrum profile is inverted due to the negative dispersion of the diffractive surface. All solutions showed a steady loss in off-axis performance due to astigmatism, which cannot be corrected in simple lenses located at the aperture stop.

6 Discussion

We observed that it is possible to correct axial color for GRIN, diffractive, and doublet designs at modest aperture values (EPD=5–15 mm). Within this range, the spherical doublet surfaces are capable of controlling spherical aberration and coma to an adequate degree. We observe better RMS performance from the doublet at these smaller apertures due to reduced secondary spectrum available from the glass solution. This is due to the greater variety of partial dispersion profiles and refractive indices presently available for selection with conventional glass.

At the full aperture of 25 mm, each correction solution is limited by different aberrations. These are apparent when one observes the transverse ray errors of each solution type (see Figure 13). The GRIN optic is limited by loss of color correction while providing some compensation through control of spherical aberration and spherochromatism. The spherical doublet no longer has the ability to control spherical aberration due to the lack of an aspheric surface. The diffractive lens controls spherical aberration and chromatic aberration well, but is limited by the secondary spectrum caused by the combination of a linear dispersion grating with a nonlinear dispersion glass. There are also practical limits to manufacturing a

diffractive component due to the fact that as the aperture expands, the zone spacing becomes progressively smaller, eventually becoming impractical. The best overall performer was the aspheric doublet, which can suppress secondary chromatic aberration and spherical aberration, being limited by a small amount of spherochromatism.

The loss of color correction for a spherical GRIN depends on two factors: the loss of surface-based correction due to the changing shape factor of the lens and the loss of correction from the GRIN transfer contributions due to the limited ΔN .

7 Challenging the F/# limits of GRIN correction

By considering the current limitations of GRIN materials, we can propose some future developments, which can offer improvements in performance. Three candidate technologies were considered:

- Negative V_{10} GRIN materials
- Increased ΔN (PVDF-PMMA-SAN17) GRIN materials
- Radial GRIN distributions

Each of these technologies were considered in turn and applied to the 25-mm EPD, 4° FOV design.

Negative V_{10} GRINs are generated by selecting a pair of compatible materials whereby the higher index material has lower dispersion than the low index material.

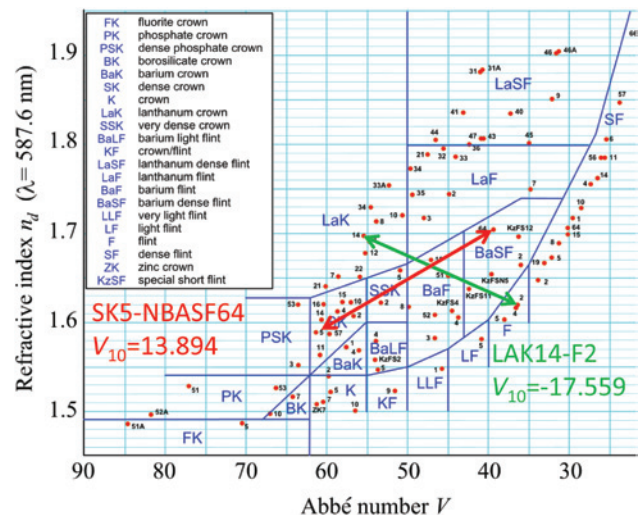


Figure 14: Illustration of both negative and positive V_{10} material combinations [4].

We recall our formula for the radial GRIN Abbé number [3]:

$$V_{10} = \frac{\Delta N_{\lambda_{mid}}}{\Delta N_{\lambda_{short}} - \Delta N_{\lambda_{long}}}$$

where ΔN represents the max index change between the two materials and λ_{long} , λ_{mid} and λ_{short} represent the short, middle, and long wavelengths of the system, respectively. Zero dispersion GRIN occurs where the ΔN is identical at long and short wavelengths, and dispersion becomes negative when the high index material is less dispersive than the lower index material. Take for example the glasses NLAK14 and F2 (shown in Figure 14). Traversing the glass chart in from top left to bottom right generates a GRIN with a negative V_{10} dispersion value of -17.559 as opposed to the opposite diagonal where a combination of SK5 and NBASF64 gives a V_{10} value of 13.894.

This approach shows particularly strong potential for aberration correction as it allows the reduction of chromatic aberration using positive power. This allows easing of the surface curvatures of the lens, which in turn reduces monochromatic aberrations. To test this hypothesis, a design was generated where the GRIN was composed of polycarbonate and a hypothetical material of equivalent dispersion characteristics to the Schott glass N-LAK7. This GRIN had a V_{10} value of -5.25 and a ΔN of 0.064. In Figure 15, we can see intuitively that the aspheric optical surfaces of the negative V_{10} design are less extreme than that of the positive V_{10} solution. This leads to reduced contributions from higher-order aberrations, which generally limit the performance of lenses at wider apertures. In Figure 16, we observe reduced axial color and spherochromatism as a result of the improved power balance.

Another effective approach toward increasing the limiting correction aperture of a GRIN is to increase the

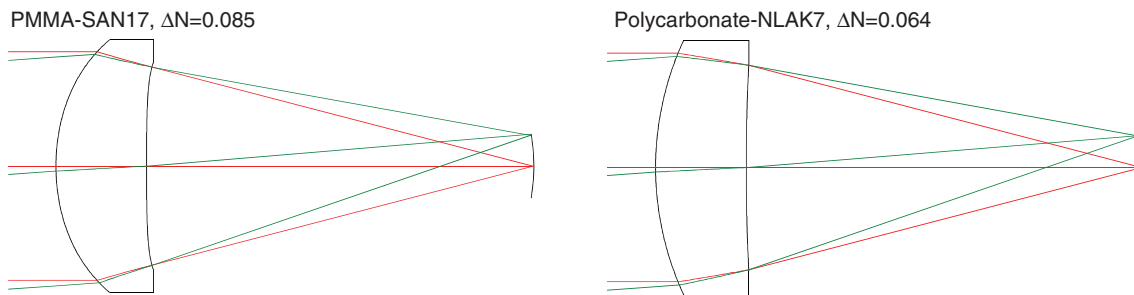


Figure 15: Optical design cross sections of positive and negative V_{10} solutions, EPD=25 mm.

Axial transverse errors (mm) of positive and negative V_{10} , 4° lenses (50 mm EFL, 25 mm EPD)

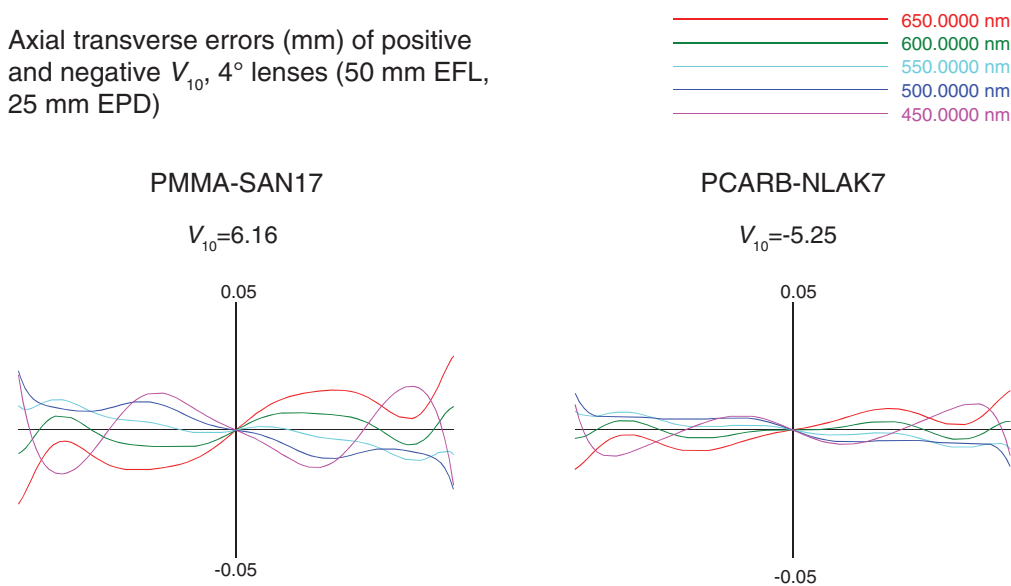


Figure 16: Transverse ray aberrations of positive and negative V_{10} , 4° FOV designs.

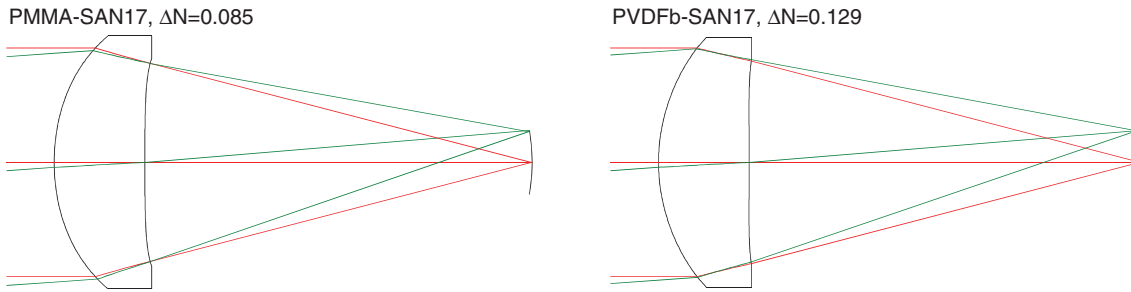


Figure 17: Optical design cross sections of PMMA-SAN17 and PVDFb-SAN17 GRINs.

Axial transverse ray errors (mm) of PMMA-SAN17 and PVDFb-SAN17 4° GRIN lenses (50 mm EFL, 25 mm EPD)

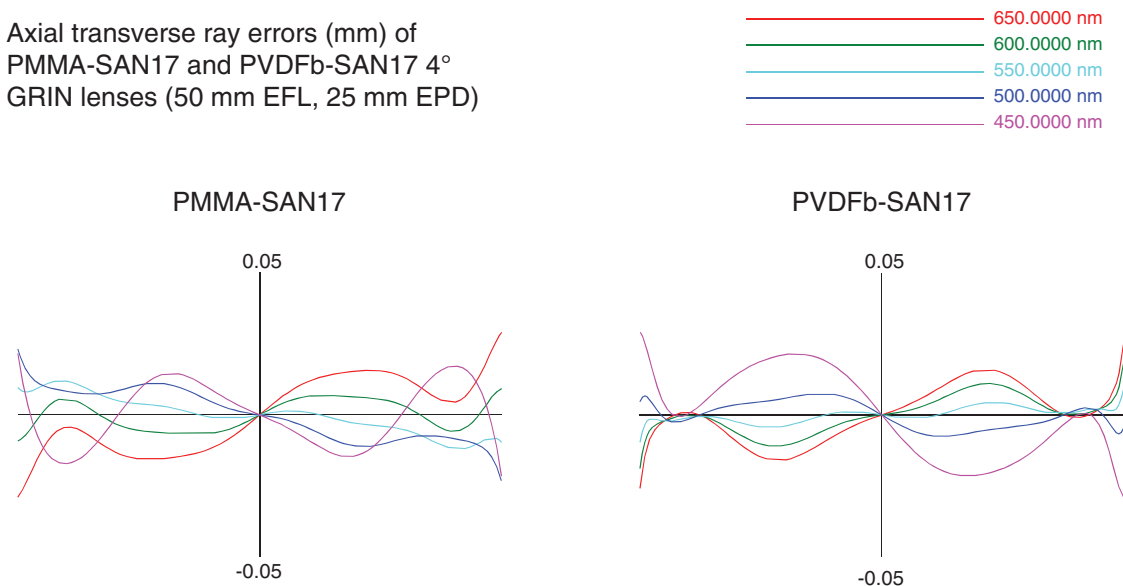


Figure 18: Transverse ray aberrations of PMMA-SAN17 and PVDFb-SAN17 4° FOV designs.

available index difference between the low and high index material. One such possibility for increased ΔN GRIN is currently under development at Polymerplus LLC. An alloy of PVDF and PMMA is used to reduce the refractive index of the low index GRIN material. Pure PVDF is a crystalline material, which is unsuitable for extrusion, but when blended correctly with PMMA forms a low index, low dispersion starting material, which may be extruded. This approach extends the ΔN to 0.129 from the 0.085 available with a PMMA-SAN17 GRIN.

Figure 17 demonstrates the effect of a larger ΔN on the optical design. In this case, our starting material on the convex first surface has lower index. This leads to this particular surface having a tighter base radius of 20.22 mm, reduced from 24.38 mm. In Figure 18, we observe the effect of this higher ΔN , lower V_{10} dispersion GRIN on image quality. The lower dispersion means the GRIN has less influence on color correction and has resulted in

increased axial color. However, this has been compensated by greater influence over the level of spherochromatism in the solution. Such a component may be useful in improving systems limited by spherochromatism, an aberration that is difficult to correct with conventional lenses.

Finally, changing the GRIN geometry inside the lens can have a significant effect upon its correction capability. In the case of our singlet components, the curvature of the spherical GRIN tends toward the tightest possible value subject to our molding rule outlined in Figure 8. This implies the GRIN needs to be more radial in nature. Radial GRINs are currently unfeasible for L-GRIN manufacture as this would require rolls of polymer with a very small radius adjacent to the optical axis, but we can, nonetheless, model the optical properties such a solution would provide.

In Figure 19, we can observe that, intuitively, the complexity of the GRIN optical surfaces has eased. The lens

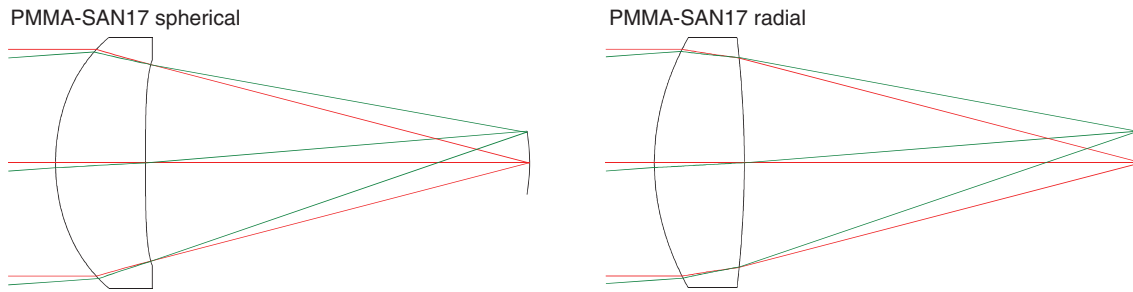


Figure 19: Optical design cross sections of PMMA-SAN17 spherical and radial GRINs, 4° FOV.

Axial transverse ray errors (mm) of PMMA-SAN17 spherical and radial GRIN lenses (50 mm EFL, 25 mm EPD)

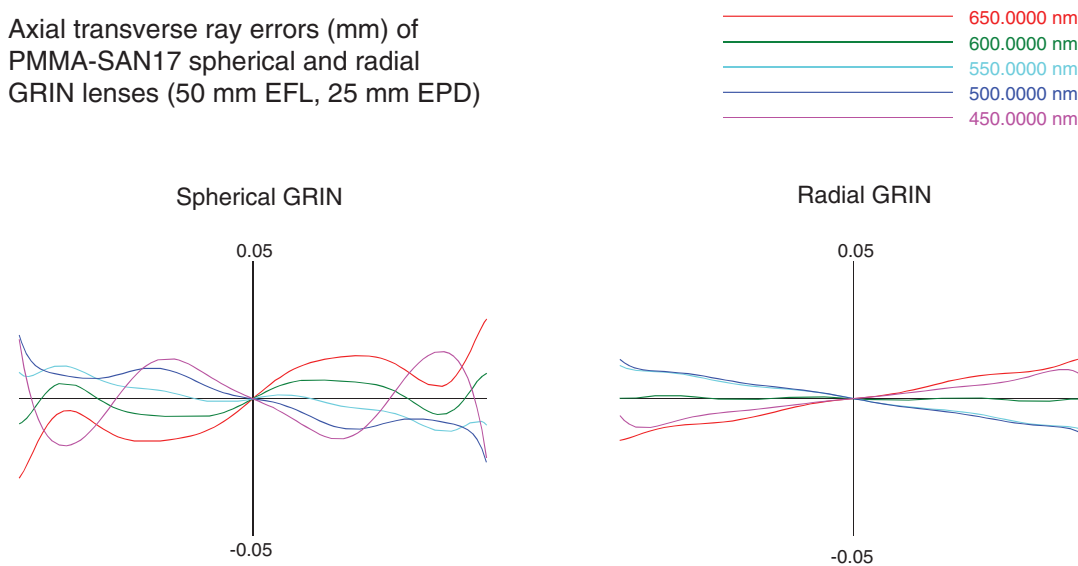


Figure 20: Transverse ray aberrations of PMMA-SAN17 spherical and radial GRINs, 4° FOV.

now consists of a bi-convex construction and has significantly reduced aspheric sag departure from the spherical GRIN solution. Surface one now departs by 0.1397 mm as opposed to 0.2250 mm on the spherical GRIN solution; surface two now departs from its base radius by 0.0398 mm as opposed to 0.2182 mm. Figure 20 demonstrates the effect of a radial profile on the transverse ray errors. We can see that the level of spherochromatism has been dramatically reduced, leaving the system limited by secondary spectrum only. This is intrinsic to the material selection of the lens; therefore, if abnormal dispersion plastics could be developed for L-GRIN materials, the level of colour correction could be improved further yet.

Radial GRINs show great potential to correct aberrations over an extended field of view; they are particularly effective in eyepiece designs where there is significant pupil separation over the lens surfaces, as demonstrated by Visconti et al. [5].

The efficacy of these next-generation GRIN technologies was then compared to current technology by evaluation of the theoretical axial RMS spot size.

In Figure 21, we observe that negative V_{10} GRIN shows the greatest aberration correction potential of the gradient index solutions. A radial GRIN of PMMA and SAN17 comes in second place, followed by a spherical GRIN of PVDFb and SAN17. The axial performance of the negative V_{10} GRIN is very close to that of an aspheric glass doublet. Significantly we notice that all GRIN solutions produce a spot size smaller than that of a diffractive surface turned onto a PMMA aspheric lens.

8 Conclusion

GRIN lenses currently offer great potential to improve optical systems in terms of a size & weight trade space.

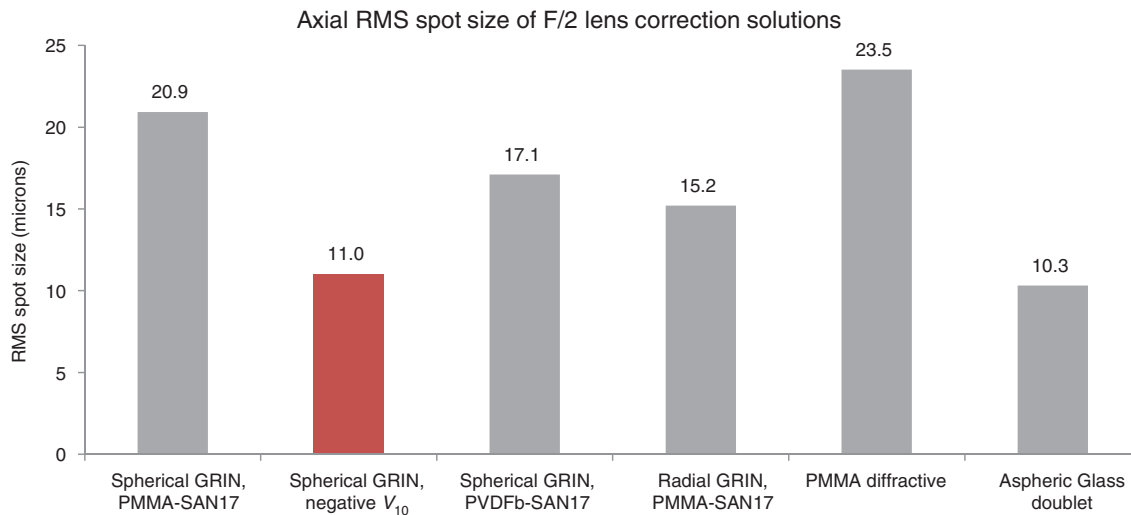


Figure 21: Comparison of axial RMS spot size for future and current aberration correction methods.

Polymer GRIN lenses give the optical designer a new degree of freedom to correct chromatic aberration within visible optical systems. It was shown that spherical GRINs composed of PMMA-SAN17 can provide comparable aberration correction to achromatic doublets or hybrid refractive-diffractive lenses. This similarity was demonstrated over a range of fields of view from 0 to 8° and a range of entrance pupil diameters from 5 to 25 mm. This GRIN correction capability currently has a natural limit in terms of $F/\#$ due to the GRIN geometry and magnitude of the ΔN and V_{10} dispersion values. Further development of the underlying polymers which form the GRIN material to incorporate negative V_{10} properties and greater ΔN values will improve this further, by allowing a greater proportion of aberration correction to take place within a single lens element. Development in this area has the potential to enable GRIN lenses to become the optical correction solution of choice for lightweight, high-performance imaging systems.

Acknowledgments: The authors would like to acknowledge Qioptiq and Polymerplus for permission to publish this work.

Statement of author contributions: Andrew Boyd as primary author wrote this manuscript. He also generated the optical designs included in this paper. Michael Ponting and Howard Fein provided the required refractive index data with which the said optical designs were completed. They also provided information on the L-GRIN process and its limitations.

References

- [1] M. Ponting, A. Hiltner, E. Baer, *Macromol. Symp.* 294, 19–32 (2010).
- [2] S. Ji, K. Yin, M. Mackey, A. Brister, M. Ponting, et al., *Opt. Eng.* 52, 112105 (2013).
- [3] F. Bociort, *J. Opt. Soc. Am A* 13, 1277–1284 (1996).
- [4] E. Bajart. Abbé diagram, adapted from Wikimedia commons.
- [5] A. J. Visconti, J. A. Corsetti, K. Fang, P. McCarthy, G. R. Schmidt, et al., *Opt. Eng.* 52, 112102 (2013).

Andrew Boyd

Qioptiq, Glascoed Road,
St Asaph, Denbighshire, LL170LL, UK,
andrew.boyd@uk.qioptiq.com

Andrew Boyd received his MSci in Physics from the University of Durham in 2008. Since 2009, he has worked as an optical designer at Qioptiq, St Asaph. His research interests are in a wide range of optical imaging systems, with a particular interest in gradient index optics.

Howard Fein

Polymerplus Inc., 7700 Hub Parkway,
Valley View, OH 44125, USA

Howard Fein has over 35 years of experience as a working scientist in diverse fields of advanced optics and design, optical and holographic interferometry, nondestructive structural and vibration analysis and applications, digital imaging and machine vision, medical and microscopic imaging, laser development and applications, optical testing, metrology, and radiation measurement. He is an internationally respected authority in holographic-interferometry and author of over 40 technical articles, invited papers, and book chapters in that field. His current work includes new applications

employing innovative design of advanced Polymer Nano-Layer Gradient Index optical materials in DOD-related programs supported by DARPA, ONR, NRL, and AFRL. He is an inventor and co-inventor on 26 current patents and over five pending patents and co-patents in LIDAR optics, digital imaging, machine vision, and optical metrology.

Michael Ponting

Polymerplus Inc., 7700 Hub Parkway,
Valley View, OH 44125, USA

Michael Ponting received a PhD from Case Western Reserve University Department of Chemical Engineering in 2010. His

current research efforts are focused on developing manufacturing processes for nanolayered polymer technologies including custom polymeric nanolayered gradient refractive index optics lens through PolymerPlus LLC. Additional research interests include polymer processing of micro- and nanolayered polymer systems, polymer structure-property relationships, and nanoscale-induced polymer optical properties.